Diffusion-Induced Chaos in Reaction Systems

Yoshiki KURAMOTO

Department of Physics, Kyoto University, Kyoto 606

A turbulent state in a distributed chemical reaction system is studied theoretically. The chaotic behavior here is basically due to the unstable growth of a spatial inhomogeneity taking place in an oscillating medium. It is argued that *phase turbulence* and *amplitude turbulence* have to be discriminated from each other according to their distinct origins. Two prototype equations describing respective types of turbulence are derived by means of some asymptotic methods, and their solutions turn out to exhibit successive bifurcations. It is found that the phase turbulence arises essentially from the interaction among a few unstable phase modes, while the amplitude turbulence may well appear in the presence of only one unstable mode which is a mixed mode of the phase and amplitude. In particular, some similarity of the amplitude turbulence to the Lorenz chaos is pointed out. Throughout the present paper, the chaotic behavior is discussed in connection with spatial pattern, so that no discrete approximations, such as a box-model or mode-truncation, are employed.

§ 1. Introduction

The possibility of diffusion-induced chemical turbulence was discussed by Kuramoto and Yamada,[1),2)] and by Rössler[3),4)] some time ago, and its experimental evidence has also appeared quite recently.[5),6)] Needless to say, a homogeneous chemical chaos such as observed in a stirred flow system[7)~9)] needs at least three nontrivial chemical components. For a diffusion-induced type of chaos, on the other hand, a two-component system well exhibits chaos, because spontaneously produced spatial inhomogeneity provides a large number of extra degrees of freedom. The significance of the statement that a two-component chaos is possible may well be realized by simply recalling the fact that people have often succeeded in abstracting complicated biochemical or ecological processes in terms of two competing species, such as activator and inhibitor, and predator and prey.

As is well known, a two-component reaction-diffusion system possesses the ability to undergo the Hopf bifurcation and/or the Turing bifurcation. It has long been overlooked, however, that the coupling between an oscillation and a spatial inhomogeneity is able to produce a spatio-temporal chaos. Which way of the above-mentioned coupling is relevant to a spatio-temporal chaos, and what is the essential origin of the complicated behavior? These are the

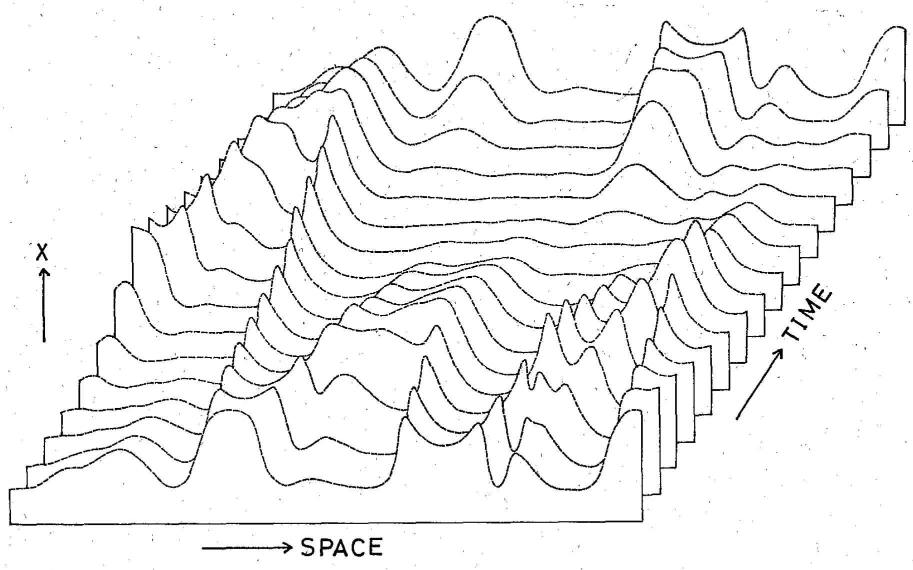

Fig. 1. (a) Chaotic concentration pattern exhibited by the Brusselator——weak turbulence case. The parameter values are: A=1.70, B=4.28, D_x=1.0, D_y=0.0 in usual notations.

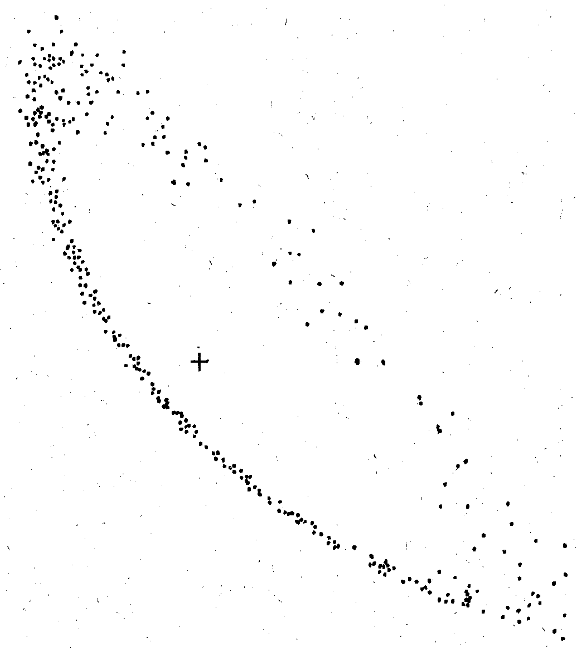

Fig. 1. (b) Distribution of the concentration states observed at various space-time points; the condition is the same as Fig. 1(a). The cross indicates the unstable focus.

problems we consider in this paper.

Figures 1 and 2 will help to get some feeling of our diffusion-induced chemical turbulence. They show some chaotic concentration patterns computer-simulated for the Brussel model,[10] where the behavior of a concentration variable X in usual notation is displayed in the space-time domain. Let us

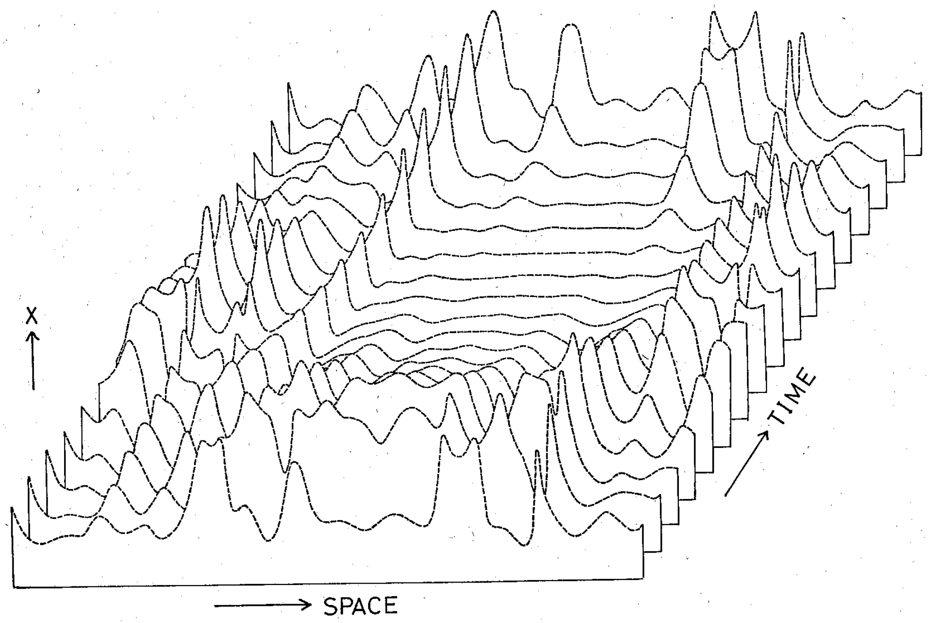

Fig. 2. (a) Chaotic concentration pattern exhibited by the Brusselator——strong turbulence case. The parameter values are: $A=2.00$, $B=5.50$, $D_x=1.0$, $D_y=0.0$.

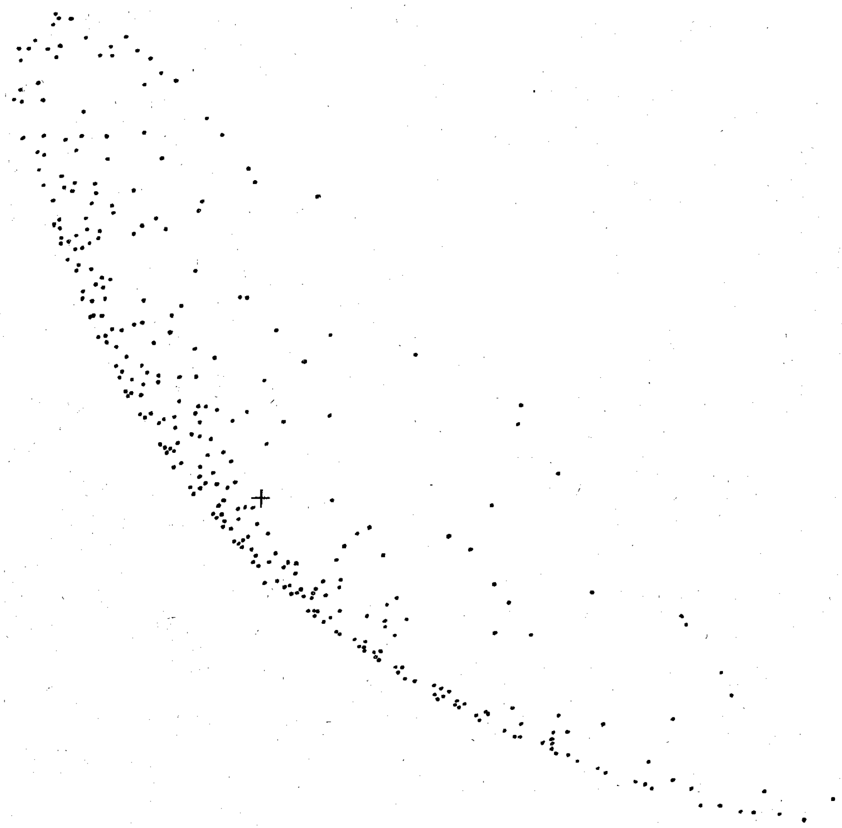

Fig. 2. (b) Distribution of the concentration states observed at various space-time points; the condition is the same as Fig. 2(a).

look into Fig. 1(a), and watch how a *local* concentration behaves in time. Then it is noticed that X undergoes quite a regular oscillation. The same is true for every part of the system, and the oscillation pattern is almost identical everywhere, except that the phase of the oscillation differs from point to point, thus making the concentration pattern look chaotic. The Brusselator has another concentration variable Y, and the feature as mentioned above applies also to Y. Thus we are led to the conclusion that the concentration state of every part of the system runs along an almost identical closed orbit on the X-Y plane. To see this more clearly, let us pick out arbitrarily a large number of points from the space-time domain of Fig. 1(a), and mark the corresponding concentration states on the X-Y plane. The distribution of the points thus obtained is shown in Fig. 1(b), where we perceive a fairly well-defined closed orbit. Since the chaotic behavior here seems to come almost entirely from the chaotic behavior of the phase, the term *phase turbulence* will be suitable for characterizing the present situation.

By changing the parameter values of the Brusselator, we find another chaotic pattern Fig. 2(a), and the corresponding distribution of the state points Fig. 2(b). The turbulence here looks stronger than the preceding one as implied by a sharper spatial variation of X in Fig. 2(a); and no well-defined orbit can be seen in Fig. 2(b). Thus such a turbulence may suitably be called *amplitude turbulence* or, probably more correctly, the coexistence of the phase and amplitude turbulences. Though such a classification of our turbulence might seem only phenomenological at this stage, we shall find later a clear distinction between the two.

The next problem we are faced with is how to separate the above-mentioned two types of turbulence from each other or, almost equivalently, how to single out their prototypes independently. It seems that the phase turbulence is more accessible than the amplitude turbulence because, as the above computer simulation implies, the phase turbulence emerges as soon as a homogeneous limit cycle oscillation loses its stability with respect to an inhomogeneous disturbance. Let us thus begin with the study of the phase turbulence.

§ 2. Phase turbulence

(A) *Onset of the phase turbulence*

Let us first study how a spatially homogeneous oscillation loses stability. The formal stability analysis is a simple matter to do. We start with the reaction-diffusion equation of a n-component system described by

$$\dot{\boldsymbol{X}}(\boldsymbol{z}, t) = \boldsymbol{F}(\boldsymbol{X}) + \widehat{D}\nabla^2\boldsymbol{X}, \tag{2·1}$$

where $\boldsymbol{X}(\boldsymbol{z}, t)$ represents a set of space-time dependent concentration variables

$(X_1, X_2, \cdots, X_n)$, and $\hat{D}$ is a diffusion matrix. The space and time coordinates are denoted by $\boldsymbol{z}$ and t throughout the present paper. Let the solution of a homogeneous limit cycle oscillation with the period T be

$$\boldsymbol{X}_0(t) = \boldsymbol{X}_0(t+T). \tag{2·2}$$

We assume throughout that $\boldsymbol{X}_0(t)$ is a stable solution of Eq. (2·1) in the absence of the diffusion term. The disturbance variable $\boldsymbol{x}(\boldsymbol{z}, t)$ around $\boldsymbol{X}_0(t)$ is defined by

$$\boldsymbol{x}(\boldsymbol{z}, t) = \boldsymbol{X}(\boldsymbol{z}, t) - \boldsymbol{X}_0(\boldsymbol{z}, t). \tag{2·3}$$

The linearization of Eq. (2·1) in $\boldsymbol{x}$ gives

$$\dot{\boldsymbol{x}} = \hat{\Gamma}(t)\boldsymbol{x} + \hat{D}\nabla^2\boldsymbol{x}, \tag{2·4}$$

where $\hat{\Gamma}(t)$ is a time-periodic matrix defined by $\Gamma_{ij}(t) = \partial F_i(\boldsymbol{X}_0)/\partial X_{0j}$. In terms of $\boldsymbol{x}(\boldsymbol{q}, t)$, which is a spatial Fourier transform of $\boldsymbol{x}(\boldsymbol{z}, t)$ with the wavevector $\boldsymbol{q}$, Eq. (2·4) may be rewritten as

$$\dot{\boldsymbol{x}}(\boldsymbol{q}, t) = \hat{\Gamma}(\boldsymbol{q}, t)\boldsymbol{x}(\boldsymbol{q}, t), \tag{2·5}$$

where

$$\hat{\Gamma}(\boldsymbol{q}, t) = \hat{\Gamma}(t) - \hat{D}q^2. \tag{2·6}$$

According to the Floquet theorem, the solution of Eq. (2·5) may generally be expressed as

$$\boldsymbol{x}(\boldsymbol{q}, t) = \hat{Q}(\boldsymbol{q}, t)\, e^{\hat{\Lambda}(\boldsymbol{q})t}\boldsymbol{x}(\boldsymbol{q}, 0), \tag{2·7}$$

where $\hat{Q}(\boldsymbol{q}, t)$ is a certain periodic matrix, and $\hat{\Lambda}$ is a time-independent characteristic matrix whose eigenvalues $\lambda_i(q)$ determine the stability of $\boldsymbol{X}_0(t)$. Let the right and left eigenvectors of $\hat{\Lambda}(\boldsymbol{q})$ be $|i, \boldsymbol{q}\rangle$ and $\langle i, \boldsymbol{q}|$, $i = 1, 2, \cdots, n$, which satisfy

$$\begin{aligned} \hat{\Lambda}|i, \boldsymbol{q}\rangle &= \lambda_i(q)\,|i, \boldsymbol{q}\rangle, \\ \langle i, \boldsymbol{q}|\hat{\Lambda} &= \langle i, \boldsymbol{q}|\lambda_i(q), \end{aligned} \tag{2·8}$$

and the orthonormality condition

$$\langle i, \boldsymbol{q}|j, \boldsymbol{q}\rangle = \delta_{i,j}. \tag{2·9}$$

the damping rates $\gamma_i(q)$ of the normal modes are defined by

$$\gamma_i(q) = -\mathrm{Re}\,\lambda_i(q). \tag{2·10}$$

Any $\gamma_i(0)$ should be non-negative, since by assumption $\boldsymbol{X}_0(t)$ is stable with respect to a homogeneous disturbance. However, there is in general one eigenvalue $\lambda_n(0)$ which is exactly zero, because any autonomous oscillation should

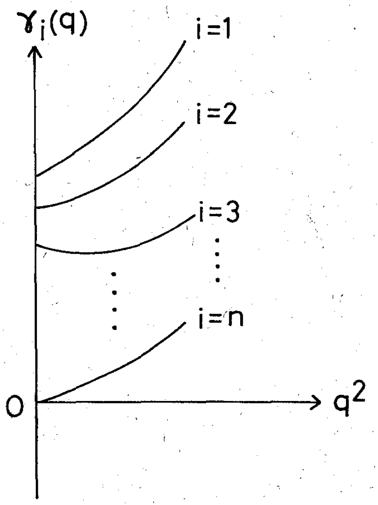

Fig. 3. Schematic dispersion curves for a small disturbance around a limit cycle oscillation. $\gamma_i(q)$ denotes the damping constant of the i-th branch, and q the wavenumber. The lowest branch $\gamma_n(q)$ is the phase-like branch for which $\gamma_n(0)=0$; the other $n-1$ branches are amplitude branches.

be neutrally stable with respect to a phase disturbance. Thus a schematic behavior of $\gamma_i(q)$ as a function of q^2 will be like Fig. 3. The lowest branch $\gamma_n(q)$ may be called *phase-like branch*, and the other branches *amplitude-like branches*. Of course, these terms become meaningless for too large q^2.

It is obvious that for sufficiently small q^2 the amplitude modes remain stable, while the stability of the phase mode depends crucially on the slope of $\gamma_n(q)$ at $q^2=0$. In other words, if one makes an expansion

$$\gamma_n(q) = \nu q^2 + \lambda q^4 + \cdots ,$$

the sign of ν determines the stability of $\boldsymbol{X}_0(t)$ with respect to a phase disturbance of slow spatial variation. The quantity ν may be called phase diffusion constant. It is easy to find the expression for ν by treating $\widehat{D}q^2$ in Eq. (2·6) as a small perturbation.[11] We find

$$\nu = \frac{1}{T}\int_0^T dt \langle n, 0|\widehat{Q}(t)^{-1}\widehat{D}\widehat{Q}(t)|n, 0\rangle . \qquad (2\cdot 11)$$

From what has been discussed so far, one may expect that a negative ν leads to a turbulence; in particular, if ν is slightly negative, then we shall have a phase turbulence.

The expression (2·11) is quite useful for practical purposes, because once a model equation has been set up, it is a simple matter to calculate ν with the help of a computer; so that one may easily find the parameter region in which the system is turbulent. In fact the turbulence of the Brusselator as shown in § 1 has been discovered in this way.[12] The expression (2·11) clearly shows that ν is eual to D if all the diffusion constants have the same value D. Therefore, the difference among diffusion constants is necessary for obtaining turbulence.

(B) *The first asymptotic method*

We have now to inquire more deeply into the origin of the phase turbulence. For this purpose it is desirable to construct a theory which does not depend upon specific models. The asymptotic method developed below, which is applicable to the limiting case $\nu \to -0$, will answer this purpose. In this limiting case, the equation of motion assumes a model-independent universal form, so that the turbulence described by such an equation may be called *ideal phase turbulence.* Though some results of our asymptotic method was already used in a previous paper,[12] the present paper is the first to give its detailed account.

For small enough q, the damping rate of the phase mode has been found to be

$$\gamma = \nu q^2 + \lambda q^4 . \tag{2·12}$$

Let us assume that ν is slightly negative and λ is a positive quantity of the order 1. Then the maximum growth rate of the phase mode is attained by the wavenumber

$$q_c \sim |\nu|^{1/2} , \tag{2·13}$$

so that the phenomenon under consideration will be characterized by the length scale

$$R_c = q_c^{-1} \sim |\nu|^{-1/2} . \tag{2·14}$$

It should also be noted that, other than the time scale of the oscillation period T, we have now another characteristic time scale

$$t_c = \gamma(q_c)^{-1} \sim |\nu|^{-2} . \tag{2·15}$$

Equation (2·14) implies that the effect of diffusion may be treated as a small perturbation, because

$$\nabla^2 \boldsymbol{X}(\boldsymbol{z}, t) \simeq \nabla^2 \boldsymbol{X}(\boldsymbol{z}/R_c, t) \sim R_c^{-2} \sim \nu . \tag{2·16}$$

The fact that the diffusion gives rise to only a small effect implies that the motion of the concentration vector $\boldsymbol{X}$ for any $\boldsymbol{z}$ is close to the limit cycle oscillation $\boldsymbol{X}_0(t+\phi)$, where the phase ϕ is nearly constant in time but may depend on $\boldsymbol{z}$. In general, there exist a small deviation of $\boldsymbol{X}$ from the limit cycle orbit $\boldsymbol{X}_0$, and also a slow time-dependence of ϕ. Thus we express $\boldsymbol{X}(\boldsymbol{z}, t)$, without approximation, as

$$\boldsymbol{X}(\boldsymbol{z}, t) = \boldsymbol{X}_0(\psi(\boldsymbol{z}, t)) + \boldsymbol{x}(\boldsymbol{z}, t) , \tag{2·17}$$

$$\psi(\boldsymbol{z}, t) = t + \phi(\boldsymbol{z}, t) , \tag{2·18}$$

where $\boldsymbol{x}$ and $\partial\phi/\partial t$ are considered to be small as far as $|\nu|$ is small. The above decomposition of $\boldsymbol{X}$ into $\boldsymbol{X}_0$ and $\boldsymbol{x}$ is made unique by choosing the phase disturbance ϕ in such a way that $\boldsymbol{x}$ may not contain the phase disturbance and represent only the net amplitude disturbance measured from the phase point ψ on the limit cycle orbit (see Appendices for further details). One may notice that the above representation of $\boldsymbol{X}$ under small $\boldsymbol{x}$ and $\partial\phi/\partial t$ is in nice accord with our picture of the phase turbulence as discussed in connection with Fig. 1.

Since the amplitude disturbance $\boldsymbol{x}$ is a rapidly decaying disturbance, we can now apply the *slaved-mode principle* of Haken,[13] whcih allows us to express $\boldsymbol{x}$ as a functional of the phase function ψ:

$$\boldsymbol{x}(\boldsymbol{z}, t) = \boldsymbol{x}(\psi, \nabla^2\psi, (\nabla\psi)^2, \cdots). \tag{2·19}$$

The above expression must not contain any odd derivative like $\nabla\psi$, $\nabla\psi\nabla^2\psi$ or $\nabla^3\psi$, because the original equation (2·1) is invariant under $\nabla\to-\nabla$. Another small quantity $\dot{\phi}$ will generally be a functional of ψ and $\boldsymbol{x}$, which means that $\dot{\phi}$ is also a functional of ψ only:

$$\dot{\phi}(\boldsymbol{z}, t) = \dot{\phi}(\psi, \nabla^2\psi, (\nabla\psi)^2, \cdots). \tag{2·20}$$

The expressions (2·19) and (2·20) are now expanded formally in powers of ∇:

$$\boldsymbol{x} = \boldsymbol{x}_1^{(1)}(\psi)\nabla^2\psi + \boldsymbol{x}_1^{(2)}(\psi)(\nabla\psi)^2 + \cdots, \tag{2·21}$$

$$\dot{\phi} = \Omega_1^{(1)}(\psi)\nabla^2\psi + \Omega_1^{(2)}(\psi)(\nabla\psi)^2 + \cdots. \tag{2·22}$$

Note that the above expansion forms have a correct limit $\boldsymbol{x}, \dot{\phi}\to 0$ as $\nabla\to 0$, namely, $\boldsymbol{X}$ approches a uniform limit cycle oscillation $\boldsymbol{X}_0(t+\phi_0)$ with a constant ϕ_0 in the absence of spatial inhomogeneity.

In Appendix A, a method by which the coefficients $\boldsymbol{x}_1^{(1)}(\psi)$, $\boldsymbol{x}_1^{(2)}(\psi)$, $\cdots$, $\Omega_1^{(1)}(\psi)$, $\Omega_1^{(2)}(\psi)$, $\cdots$ are determined is shown; and all these quantities will turn out periodic in ψ with the period T in the limit $\psi\to\infty$ or, equivalently, $t\to\infty$. Let us now concentrate on Eq. (2·22) which is the only important equation for the argument below. Equation (2·22) may be rewritten as

$$\dot{\phi} = \Omega_1^{(1)}(t+\phi)\nabla^2\phi + \Omega_1^{(2)}(t+\phi)(\nabla\phi)^2 + \cdots. \tag{2·23}$$

Since the characteristic time scale of ϕ has been expected to be $t_c\sim\nu^{-2}$, which is much longer than T, the coefficients $\Omega_1^{(1)}$, $\Omega_1^{(2)}$, $\cdots$ in Eq. (2·23) may safely be time-averaged. Thus we obtain

$$\dot{\phi} = \nu\nabla^2\phi + \mu(\nabla\phi)^2 + \cdots \tag{2·24}$$

with

$$\nu = \frac{1}{T}\int_0^T dt\langle n, 0|\hat{Q}(t)^{-1}\hat{D}\hat{Q}(t)|n, 0\rangle, \tag{2·25a}$$

$$\mu=\frac{1}{T}\int_0^T dt\langle n,0|\widehat{Q}(t)^{-1}\widehat{D}\frac{d}{dt}\widehat{Q}(t)|n,0\rangle \tag{2·25b}$$

as shown by Appendix A. Note that (2·25a) is identical to (2·11) as it should be; why ν is termed *phase diffusion constant* has become even clearer in the form of (2·24).

Among various terms in Eq. (2·24), only the most dominant terms in the limit $|\nu|\to 0$ are now taken into account. This has been done in Appendix B, and the result is

$$\dot{\phi}=\nu\nabla^2\phi+\lambda\nabla^2\nabla^2\phi+\mu(\nabla\phi)^2 . \tag{2·26}$$

Under a suitable scaling of t, $\boldsymbol{z}$ and ϕ, the coefficients ν, λ and μ are normalized. Thus, assuming $\nu<0$ and $\lambda>0$, we finally obtain a parameter-free equation

$$\dot{\phi}=-\nabla^2\phi+\nabla^2\nabla^2\phi+(\nabla\phi)^2 . \tag{2·27}$$

For later purposes, we rewrite Eq. (2·27) in terms of $\boldsymbol{v}$ defined by

$$\boldsymbol{v}=\nabla\phi \tag{2·28}$$

as

$$\dot{\boldsymbol{v}}=-\nabla^2\boldsymbol{v}+\nabla^2\nabla^2\boldsymbol{v}+2\boldsymbol{v}\cdot\nabla\boldsymbol{v} ,$$

$$\mathrm{Curl}\,\boldsymbol{v}=0 . \tag{2·29}$$

Note that Eq. (2·29) looks somewhat like the Navier-Stokes equation for a potential flow with negative viscosity. The above equation is the basic equation with which an ideal phase turbulence is discussed below.

(C) *Successive bifurcations*

If the system size is large enough, a computer simulation shows that the solution of Eq. (2·29) or Eq. (2·27) behaves chaotically in space and time.[1] We will now investigate in detail how a chaotic state eventually comes out through successive bifurcations. For this purpose, we study a small system in which only a few modes are unstably excited. (See Fig. 4.)

For the sake of simplicity, we consider a one-dimensional system of length L with a periodic boundary condition. Then it is easy to see that the quantity

$$v_0=\frac{1}{L}\int_0^L v(z,t)\,dz \tag{2·30}$$

is a constant of motion. Therefore, whether the solution of Eq. (2·29) may be chaotic or non-chaotic, we have a one-parameter family of solutions $v=v(z, t;v_0)$ parametrized by v_0. We now split v into the uniform and nonuniform parts:

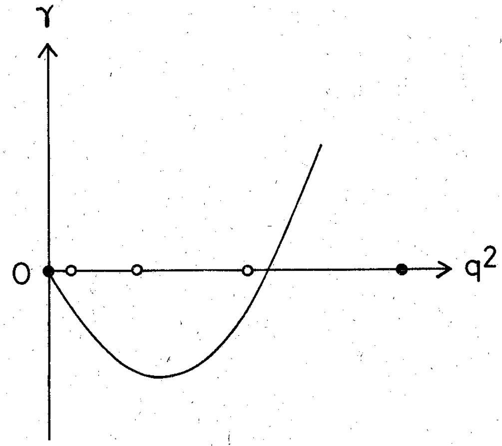

Fig. 4. Damping constant γ of the phase-like branch vs q^2 for $\nu<0$. For a finite system, q takes on discrete values. Unstable modes are indicated by open circles on the q^2-axis.

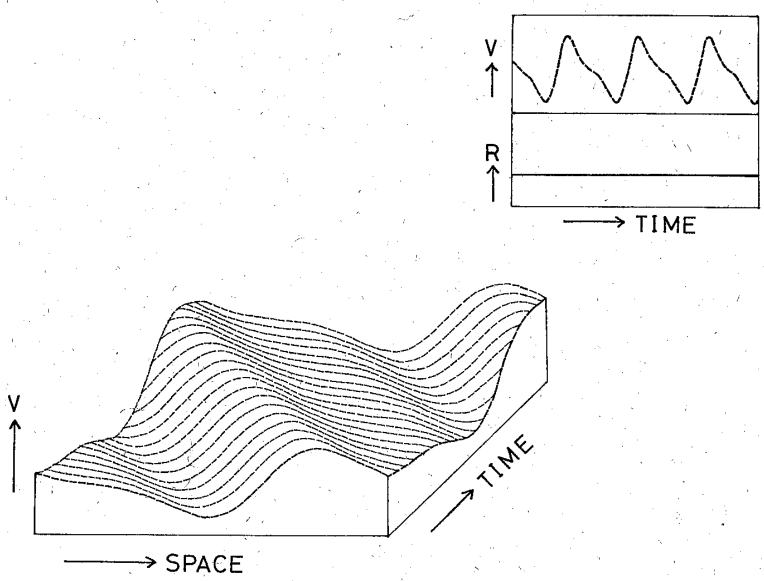

Fig. 5. Pattern of the phase gradient in the space-time domain for $L=10.0$. $v(z, t)$ at fixed z shows an oscillation, while R defined by (2.32) remains constant.

$$v=v_0+v'(z, t; v_0). \tag{2·31}$$

If $\nu>0$, then $v'=0$ is a stable state. Namely, we have a one-parameter family of stable solutions $v=v_0$ or $\phi=v_0z+v_0^2t$. These solutions represent travelling plane waves if interpreted in terms of the concentration variables. The existence of such a family of plane waves was proved by Kopell and Howard[14] some years ago. If $\nu<0$, on the contrary, we must have a nonvanishing v'; and if v' is chaotic we have a one-parameter family of phase-turbulent states.

Let us now fix the value of v_0 as $v_0=0.5$, and change L from small to large, thus increasing the number of linerly unstable modes. For $L=10.0$ there exists only one unstable mode. The space-time pattern of v for this case is shown in Fig. 5. It is observed that a wave is propagating with a constant velocity and a constant waveform. This means that one observes *locally* and oscillation of v, while the global quantity R defined by

$$R=\frac{1}{L}\int_0^L v(z)^2 dz \tag{2·32}$$

remains constant in time.

Let the system size be $L=13.2$ (see Fig. 6). We have now two linearly unstable modes. Again a propagating wave with a constant velocity is observed. However, the waveform is changing in time periodically, and this period looks independent of the period associated with the successive arrival of the waves at some z. Thus a quasiperiodic behavior of v is observed locally, while R exhibits a simple periodic motion.

Finally we consider the case $L=20.0$, for which three unstable modes are excited. Figure 7 shows that the behavior of v is already chaotic. The propagation velocity and waveforms are fluctuating in an irregular manner. We observe also the generation and absorption of waves.

It is true that the essential origin of the phase turbulence is not yet clearly seen from the study above. Though the successive bifurcations above show a strong similariy to the experimental results for Taylor vortex flow,[15),16)] a common underlying mechanism, if any, has yet to be clarified. Still we may say at least that the phase turbulence comes from the interaction among a few unstably excited waves, and at this point the phase turbulence seems to make a contrast to the amplitude turbulence discussed below where only one unstable mode well produces chaos.

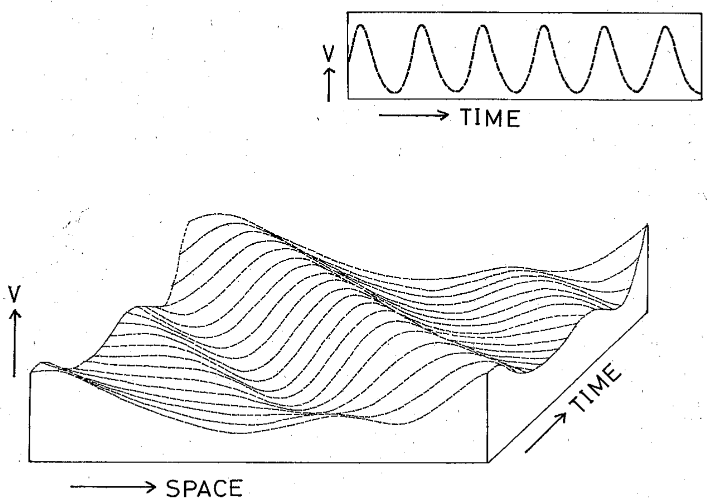

Fig. 6. Pattern of the phase gradient in the space-time domain for $L=13.2$. R exhibits an oscillation.

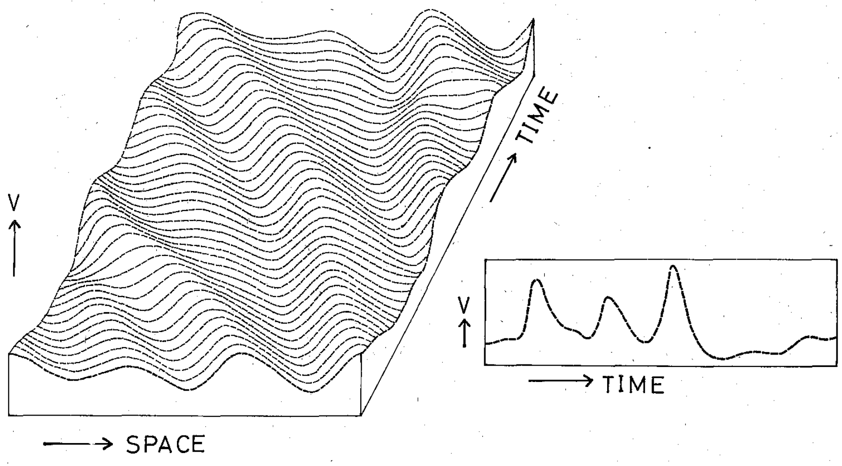

Fig. 7. Pattern of the Phase gradient in the space-time domain for $L=20.0$. The behavior of R is chaotic.

§ 3. Amplitude turbulence

For the purpose of studying an *ideal amplitude turbulence*, a powerful tool is the second asymptotic method introduced below. This asymptotic method is applicable to small amplitude oscillations which are realized slightly above the Hopf bifurcation point.

(A) *The second asymptotic method*

Since the present asymptotic method has repeatedly been discussed in the literature,[17)~22)] the explanation below is made as brief as possible. Suppose that a uniform system described by the equation,

$$\dot{\boldsymbol{X}} = \boldsymbol{F}(\boldsymbol{X}), \tag{3·1}$$

is in the vicinity of the Hopf bifurcation point. Let u and u^* be the amplitudes of a pair of the critical eigenvectors. Just at the bifurcation point, the small amplitude behavior of u is simply described by a harmonic oscillation, $u = w \cdot \exp(i\omega t)$, with an undetermined complex amplitude w. We now try to find the equation obeyed by w beyond the linear regime and also in the presence of diffusion. In a way, the problem here is how to generalize Landau's small amplitude expansion[23),24)] well known in the theory of hydrodynamic instablities. The precise form of the equation for w may be derived by means of either the reductive perturbation method[17)~20)] or the mode-coupling method.[21),22)] We find that w generally obeys the equation

$$\dot{w} = (a - c|w|^2)\, w + b\nabla^2 w\,, \tag{3·2}$$

where a, b and c are generally complex. The imaginary part of a is trivial since it only gives rise to a small correction in the critical frequency. The real part of b generally turns out positive and we assume that the real part of c is positive. The last assumption presupposes that the present bifurcation is a normal bifurcation. Thus, after making a suitable re-scaling for t, z and w, we obtain

$$\dot{w} = w - (1+ic_1)\nabla^2 w - (1+ic_2)|w|^2 w\,. \tag{3·3}$$

Without the diffusion term, the solution of Eq. (3·3) approaches a limit cycle whose orbit is a unit circle on the X-Y plane, where X and Y are the real and imaginary parts of w, respectively. The linear stability analysis of this homogeneous oscillation in the presence of the diffusion shows that the dispersion curve of the phase-like branch is given by[19]

$$\gamma(q) = 1+q^2 - [(1+q^2)^2 - 2(1+c_1c_2)q^2 - (1+c_1^2)q^4]^{1/2}\,. \tag{3·4}$$

Up to q^4, the $\gamma(q)$ above is identical to Eq. (2·12) with ν and λ given by

$$\nu = 1+c_1c_2\,,$$

$$\lambda = c_1^2(1+c_2^2)/2>0\,. \tag{3·5}$$

Therefore, Eq. (3·2) can show turbulence[1] if no special restriction is imposed upon the value of c_1 and c_2.*)

(B) *Successive bifurcations*

For large negative ν, the amplitude effect becomes quite important. This is because the unstable modes in such a case may have large wavenumbers, and then the dispersion curve (3·4) loses the character as a phase-like branch. Let us consider again a one-dimensional system with a periodic boundary condition. We make the system length so small that there is always only one unstble mode even if $|\nu|$ is large. This procedure enables us to suppress the phase turbulence, and makes it possible to study quite a new chaotic state for which the amplitude effect plays a decisive role.

Let the system size be fixed at $L=6.0$ throughout, and observe what happens as we increase $|\nu|$. Specifically, we also fix c_1 as $c_1=-2.0$ and increase c_2 from 3.7 to 4.5.

For the case $c_2=3.7$, we find an oscillating nonuniform pattern. How this pattern looks needs some explanation. At some instant t, the concentration state of the system defines a set of an infinite number of points on the X-Y plane, each point representing the (X, Y) state at each spatial point of the system. This set of points forms a segment of a line as shown in Fig. 8. We observe that the segment makes a revolution around an unstable focus at $X=Y=0$, keeping its own form unchanged and with a constant angular ve-

*) For the Brusselator, the expressions for c_1 and c_2 are:[18] $c_1=-A(D_x-D_y)/(D_x+D_y)$, $c_2=(4-7A^2+4A^4)/[3A(2+A^2)]$. Thus, there is certainly a parameter region in which ν is negative.

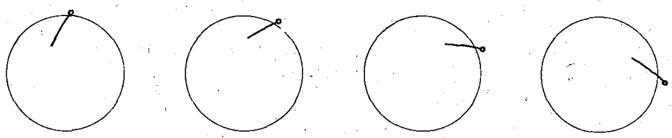

Fig. 8. Temporal behavior of the concentration state for $c_2=3.7$. Each circle indicates the reference limit cycle orbit on the X-Y plane. The segment is an abbreviated representation of an instantantaneous concentration state of the system (see the text for details). The small open circle at the end of the segment represents the state of a certain z of the system.

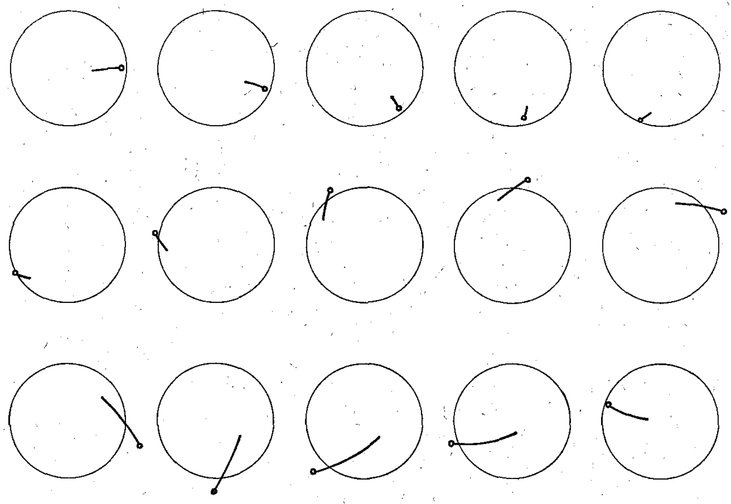

Fig. 9. Temporal behavior of the concentration state for $c_2=4.0$.

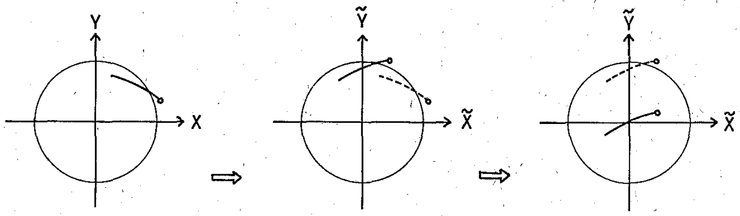

Fig. 10. Construction of the new coordinates $\tilde{X}$-$\tilde{Y}$.

locity. Therefore, if we observe the concentration pattern in a rotating state space with a suitable rotation frequency, then the pattern will look stationary. And this has actually been confirmed numerically.

Next we consider the case $c_2=4.0$. The motion of the above-mentioned segment in this case is shown in Fig. 9. The form of the segment is now changing periodically, and its period looks independent of the revolution period. In order to study how the corresponding concentration pattern looks in a rotating state space, we must introduce a precise definition of the rotating state space as follows. As is illustrated in Fig. 10, we define new coordinates $\tilde{X}$-$\tilde{Y}$ in such a way that the uniform component of the concentrations may

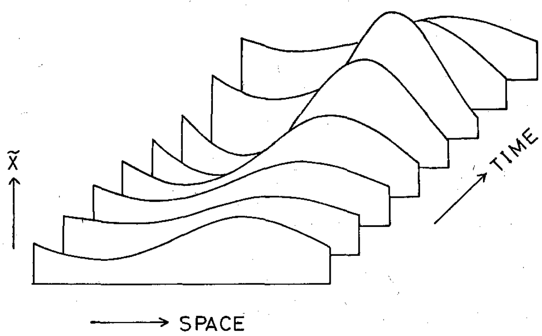

Fig. 11. Oscillating pattern of $\widetilde{X}$ for the case $c_2=4.0$. A similar behavior is also obtained for $\widetilde{Y}$.

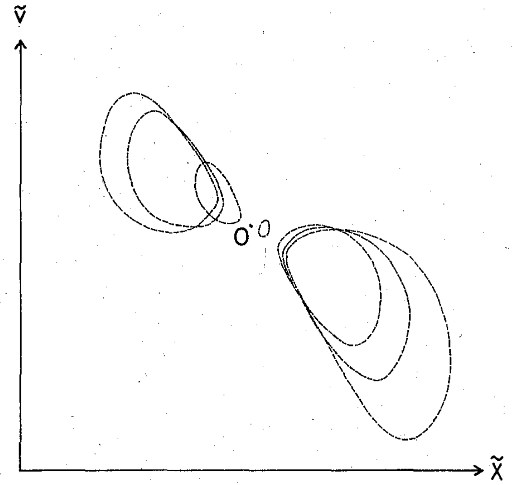

Fig. 12. Oscillations of $\widetilde{X}$ and $\widetilde{Y}$ observed at various z of the system, different orbits correspond to different z. The origin of the $\widetilde{X}$-$\widetilde{Y}$ coordinates is denoted by O.

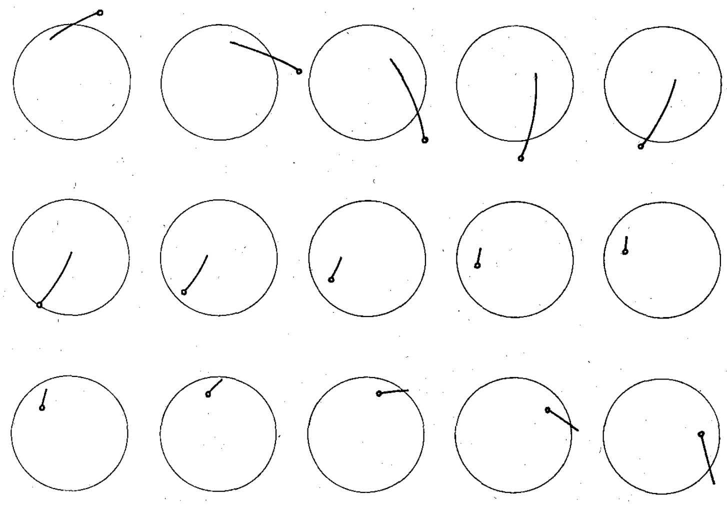

Fig. 13. Temporal behavior of the concentration state for $c_2=4.5$.

lie always on the $\widetilde{X}$ axis, and then we subtract the uniform part of $\widetilde{X}$. The final coordinates are also denoted by $\widetilde{X}$-$\widetilde{Y}$ for the sake of brevity. In the $\widetilde{X}$-$\widetilde{Y}$ representation, the pattern now exhibits a periodic vibration as shown in Fig. 11. If we observe the temporal behavior of $\widetilde{X}$ and $\widetilde{Y}$ at some z of the system, then the corresponding trajectory on the $\widetilde{X}$-$\widetilde{Y}$ plane is a limit cycle orbit like Fig. 12, where the different orbits are realized at different z of the system; in particular, the zero amplitude oscillation at the point O is realized at the nodal point of the pattern. Let us further increase c_2. Figure 13 shows the motion of the segment for $c_2=4.5$. The behavior here is quite different from the preceding one. It may be noted that the segment runs occasionally across the origin (unstable focus) and after that the head and tail

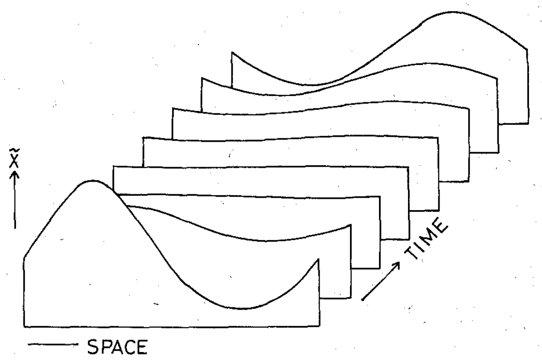

Fig. 14.(a) Flip-flop of the pattern with a long period of an intermediate state for the case $c_2=4.2$.

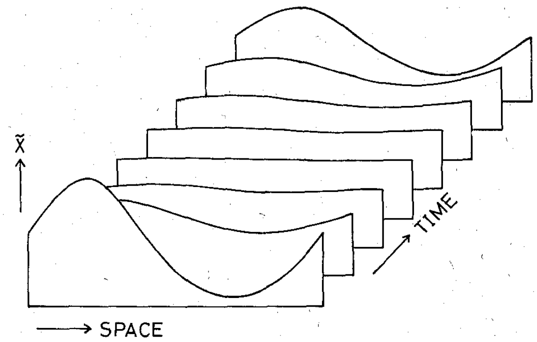

Fig. 14.(b) A slight difference in the initial condition from that of (a) makes the temporal development of the pattern quite different; the pattern here fails to make a flip-flop. $c_2=4.2$.

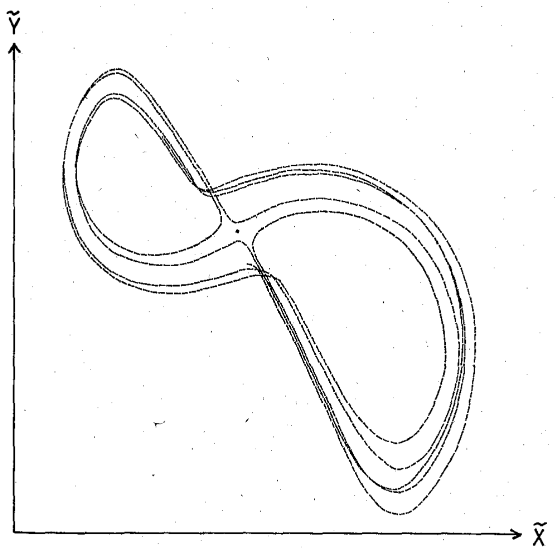

Fig. 15. Chaotic trajectory observed at a certain z of the system for the case $c_2=4.5$.

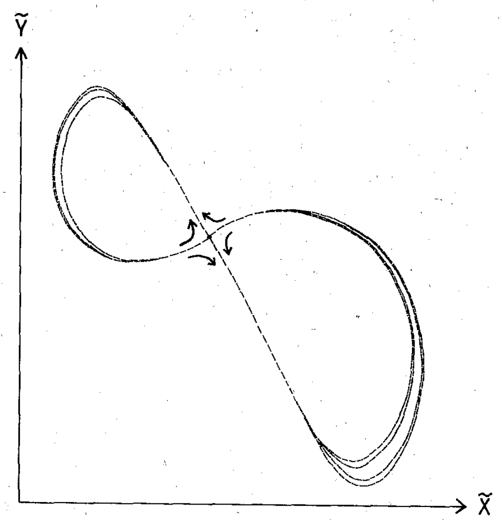

Fig. 16. Chaotic trajectory observed at a certain z of the system for the case $c_2=4.1$.

of the segment are interchanged. Each time this happens, the pattern in terms of $\tilde{X}$ and $\tilde{Y}$ makes a flip-flop as is shown in Fig. 14. More importantly, such a flip-flop motion takes place in a stochastic manner. Actually, the $\tilde{X}$-$\tilde{Y}$ trajectory observed at some z of the system is chaotic as shown in Fig. 15. One may immediately notice the similarity of our trajectory to that of the Lorenz chaos.[25),26)]

It is interesting to see how such a chaotic state bifurcates from a non-chaotic state. Figure 16 shows a nearly critical situation ($c_2=4.1$) where a chaotic motion has just started to appear. That figure implies that at the onset of our chaos two closed orbits are interlinked at the origin of the $\tilde{X}$-$\tilde{Y}$ space. We found that there is a very long period during which the state point $(\tilde{X}, \tilde{Y})$ stays in the vicinity of the point O, and that this occurs simultaneously at every z of the system. In other words, there is a very long period during which the system undergoes an almost uniform limit cycle oscillation in the original representation X–Y, in spite of the fact that such a uniform oscillation is strongly unstable.

§ 4. Conclusion and future problems

We have succeeded in extracting independently two distinct prototypes of the diffusion-induced chemical turbulence. An important problem left unsolved is how to find the connection of our chaos to some known types of chaos found so far for the systems of a few degrees of freedom.[27] Some important contributions along this line have already appeared, and they are due to Rössler,[3),4)] and Yamada and Fujisaka.[28] However, whether the box models adopted by them correctly simulate a finite distributed system has still to be examined carefully. Generally speaking, our diffusion-induced chaos appears if an oscillating system produces spontaneously a spatial inhomogeneity. Since a spatial inhomogeneity will work as a desynchronizing force, our system may have some resemblance to a system of coupled oscillators having different natural frequencies. When the spatial inhomogeneity is weak enough, the system will still be in a self-synchronized state so that the description of the concentration behavior in terms of a space-time dependent phase function makes sense. In such a case we have a phase turbulence. On the contrary, for strong enough inhomogeneity, a self-synchronized state is unable to persist. This implies the appearance of a phaseless point somewhere in the system, which leads the system to quite a new dynamic regime where the Lorenz type of chaos is a dominant feature of the system's behavior. For the intermediate strength of the inhomogeneity, there is certainly the possibility of the appearance of another type of chaos which is beyond the scope covered by our asymptotic methods. For example, if the underlying oscillation is of a strong relaxation-oscillation type, the vibration of the segment like Fig. 9 cannot even approximately be separated from the revolution of the segment itself; and the coupling between these two periodic motions might lead to a pitchfork bifurcation such as exhibited by Rössler's 2-box Rashevsky-Turing system.[3]

Acknowledgements

A part of the present work has been done during my stay at Universität Stuttgart, and I would like to express my sincere gratitude to Professor H. Haken for his kind hospitality and fruitful discussion. Thanks are also due to Professor K. Tomita and Professor O. E. Rössler for many stimulationg discussions.

Appendix A

As is mentioned in the text, the quantity $\boldsymbol{x}$ defined in Eq. (2·17) represents the amplitude disturbance measured from the phase point ψ on the limit cycle orbit $\boldsymbol{X}_0$, and hence $\boldsymbol{x}$ must not contain the phase disturbance; the phase distrubance has already been taken into account by ψ. The above statement can be formulated by expanding $\boldsymbol{x}(z, t)$ in terms of the Floquet eigenvectors,

$$\boldsymbol{x}(z, t) = \sum_{i=1}^{n} x_i(z, t)\hat{Q}(\psi)|i, 0\rangle\,, \tag{A·1}$$

and then requiring $x_n(z, t)$ to be identically zero. For the same reason, the quantities $\boldsymbol{x}_l^{(m)}(\psi)$ defined by Eq. (2·21) should not contain the phase component, namely

$$\boldsymbol{x}_l^{(m)}(\psi) = \sum_{i=1}^{n-1} x_{li}^{(m)}(\psi)\hat{Q}(\psi)|i, 0\rangle. \tag{A·2}$$

Equation (2·17) together with the expansion for $\boldsymbol{x}$ given by Eq. (2·21) are now substituted into Eq. (2·1), yielding

$$\begin{aligned}
&\frac{d\boldsymbol{X}_0}{d\psi}\dot{\psi} + \frac{d\boldsymbol{x}_1^{(1)}}{d\psi}\dot{\psi}\cdot\nabla^2\psi + \boldsymbol{x}_1^{(1)}\nabla^2\dot{\psi} + \frac{d\boldsymbol{x}_1^{(2)}}{d\psi}\dot{\psi}\cdot(\nabla\psi)^2 \\
&\quad + 2\boldsymbol{x}_1^{(2)}\nabla\psi\nabla\dot{\psi} + \cdots \\
&\quad = \boldsymbol{F}(\boldsymbol{X}_0) + \hat{\Gamma}(\psi)\{\boldsymbol{x}_1^{(1)}\nabla^2\psi + \boldsymbol{x}_1^{(2)}(\nabla\psi)^2 + \cdots\} \\
&\quad + \hat{D}\left\{\frac{d\boldsymbol{X}_0}{d\psi}\nabla^2\psi + \frac{d^2\boldsymbol{X}_0}{d\psi^2}(\nabla\psi)^2 + \cdots\right\} + O(\boldsymbol{x}^2).
\end{aligned} \tag{A·3}$$

The expression (2·22) is now substituted into (A·3). Then the both sides of Eq. (A·3) may be expressed only in terms of ψ and its various spatial derivatives. After rearangement, Eq. (A·3) reduces to the form

$$\boldsymbol{f}_0(\psi) + \boldsymbol{f}_1^{(1)}(\psi)\nabla^2\psi + \boldsymbol{f}_1^{(2)}(\psi)(\nabla\psi)^2 + \cdots = 0\,, \tag{A·4}$$

where

$$\boldsymbol{f}_0(\psi) = \frac{d\boldsymbol{X}_0(\psi)}{d\psi} - \boldsymbol{F}(\boldsymbol{X}_0(\psi)), \tag{A·5a}$$

$$\boldsymbol{f}_1^{(1)}(\psi) = \frac{d\boldsymbol{x}_1^{(1)}(\psi)}{d\psi} - \hat{\Gamma}(\psi)\boldsymbol{x}_1^{(1)}(\psi) + \boldsymbol{g}_1^{(1)}(\psi), \tag{A·5b}$$

$$\boldsymbol{f}_1^{(2)}(\psi) = \frac{d\boldsymbol{x}_1^{(2)}(\psi)}{d\psi} - \hat{\Gamma}(\psi)\boldsymbol{x}_1^{(2)}(\psi) + \boldsymbol{g}_1^{(2)}(\psi), \tag{A·5c}$$

$$\cdots\cdots\cdots$$

with

$$\boldsymbol{g}_1^{(1)}(\psi) = \frac{d\boldsymbol{X}_0(\psi)}{d\psi}\Omega_1^{(1)}(\psi) - \hat{D}\frac{d\boldsymbol{X}_0(\psi)}{d\psi}, \tag{A·6a}$$

$$\boldsymbol{g}_1^{(2)}(\psi) = \frac{d\boldsymbol{X}_0(\psi)}{d\psi}\Omega_1^{(2)}(\psi) - \hat{D}\frac{d^2\boldsymbol{X}_0(\psi)}{d\psi^2}. \tag{A·6b}$$

For Eq. (A·4) identically to hold, we must require that all $\boldsymbol{f}_l^{(m)}(\psi)$ should identically be zero. The first equation $\boldsymbol{f}_0(\psi)=0$ is automatically satisfied because $\boldsymbol{X}_0(t)$ is a solution of $\dot{\boldsymbol{X}}_0(t)=\boldsymbol{F}(\boldsymbol{X}_0(t))$. If we expand $\boldsymbol{f}_l^{(m)}(\psi)$ as

$$\boldsymbol{f}_l^{(m)}(\psi) = \sum_{i=1}^{n} f_{li}^{(m)}(\psi)\hat{Q}(\psi)|i,0\rangle, \tag{A·7}$$

the other equations, $\boldsymbol{f}_l^{(m)}(\psi)=0$, become

$$f_{li}^{(m)}(\psi) = \frac{dx_{li}^{(m)}(\psi)}{d\psi} - \lambda_i x_{li}^{(m)}(\psi) + g_{li}^{(m)}(\psi) = 0, \tag{A·8}$$

where $g_{li}^{(m)}(\psi)$ is defined by

$$\boldsymbol{g}_l^{(m)}(\psi) = \sum_{i=1}^{n} g_{li}^{(m)}(\psi)\hat{Q}(\psi)|i,0\rangle. \tag{A·9}$$

Since $x_{ln}^{(m)}(\psi)=0$ according to (A·2), Eq. (A·8) is equivalent to

$$x_{li}^{(m)}(\psi) = e^{\lambda_i\psi}\left\{x_{li}^{(m)}(0) - \int_0^{\psi} e^{-\lambda_i\psi'} g_{li}^{(m)}(\psi')\,d\psi'\right\} \quad (i \neq n) \tag{A·10}$$

and

$$g_{ln}^{(m)}(\psi) = 0. \tag{A·11}$$

From Eqs. (A·10) and (A·11), all the coefficients $x_{li}^{(m)}(\psi)$ and $\Omega_l^{(m)}(\psi)$ may in principle be determined. In particular, the explicit forms of $x_{1i}^{(1)}(\psi)$, $x_{1i}^{(2)}(\psi)$, $\Omega_1^{(1)}(\psi)$ and $\Omega_1^{(2)}(\psi)$ are easy to find. For finding these we must use the property:

$$\frac{d\boldsymbol{X}_0(\psi)}{d\psi} = v\cdot\hat{Q}(\psi)|n,0\rangle, \tag{A·12}$$

where v is a certain constant. The proof of (A·12) is given at the end of this appendix. Equation (A·12) is now substituted into (A·6a) and (A·6b), and noting Eq. (A·9) we obtain

$$g_{1i}^{(1)} = v\{\delta_{in}\Omega_1^{(1)}(\psi) - \langle i,0|\hat{Q}(\psi)^{-1}\hat{D}\hat{Q}(\psi)|n,0\rangle\}, \tag{A·13a}$$

$$g_{1i}^{(2)} = v\left\{\delta_{in}\Omega_1^{(2)}(\psi) - \langle i,0|\hat{Q}(\psi)^{-1}\hat{D}\frac{d}{d\psi}\hat{Q}(\psi)|n,0\rangle\right\}. \tag{A·13b}$$

Thus the condition (A·11) for $l=1$ becomes

$$\Omega_1^{(1)}(\psi) = \langle n,0|\hat{Q}(\psi)^{-1}\hat{D}\hat{Q}(\psi)|n,0\rangle, \tag{A·14a}$$

$$\Omega_1^{(2)}(\psi)=\langle n,0|\widehat{Q}(\psi)^{-1}\widehat{D}\frac{d}{d\psi}\widehat{Q}(\psi)|n,0\rangle\,. \tag{A·14b}$$

Substituting the expressions (A·13a) and (A·13b) into Eq. (A·10), and taking the limit $\psi\to\infty$, we find

$$x_{1i}^{(1)}(\psi)=\lim_{\psi\to\infty}\int_0^{\psi}e^{\lambda_i(\psi-\psi')}\langle i,0|\widehat{Q}(\psi)^{-1}\widehat{D}\widehat{Q}(\psi)|n,0\rangle\,, \tag{A·15a}$$

$$x_{1i}^{(2)}(\psi)=\lim_{\psi\to\infty}\int_0^{\infty}e^{\lambda_i(\psi-\psi')}\langle i,0|\widehat{Q}(\psi)^{-1}\widehat{D}\frac{d}{d\psi}\widehat{Q}(\psi)|n,0\rangle\,. \tag{A·15b}$$

Since $\widehat{Q}(\psi)$ is periodic in ψ, the four coefficients above are also periodic in ψ. Other coefficients are found by iteration, and hence all the coefficients must be periodic for $\psi\to\infty$.

Proof of (A·12):

Differentiation of the equation $\boldsymbol{f}_0(\psi)=0$ with respect to ψ gives

$$\left[\frac{d}{d\psi}-\widehat{\Gamma}(\boldsymbol{X}_0(\psi))\right]\frac{d\boldsymbol{X}_0(\psi)}{d\psi}=0\,, \tag{A·16}$$

which shows that the quantity $d\boldsymbol{X}_0(\psi)/d\psi$ satisfies the linear disturbance equation $\dot{\boldsymbol{x}}=\widehat{\Gamma}(\boldsymbol{X}_0)\boldsymbol{x}$. Thus the solution of (A·16) can generally be expressed as

$$\begin{aligned}\frac{d\boldsymbol{X}_0(\psi)}{d\psi}&=\sum_{i=1}^{n}X_{0i}(\psi)\widehat{Q}(\psi)|i,0\rangle\\&=\sum_{i=1}^{n}e^{\lambda_i\psi}X_{0i}(0)\widehat{Q}(\psi)|i,0\rangle\,.\end{aligned} \tag{A·17}$$

Since $d\boldsymbol{X}_0(\psi)/d\psi$ is periodic in ψ, all $X_{0i}(0)$ except $i=n$ should vanish. Thus we have (A·12) with

$$v=X_{0n}(0)=\left|\frac{d\boldsymbol{X}_0(t)}{dt}\right|_{t=0}. \tag{A·18}$$

Appendix B

In this appendix, the most dominant terms are selected out of various terms in Eq. (2·24). As was mentioned in § 2, the space-time dependence of ϕ is characterized by the characteristic scales $R_c\sim|\nu|^{-1/2}$ and $t_c\sim\nu^{-2}$. This implies that ϕ has the following scaling form:

$$\begin{aligned}\phi&=\phi(\boldsymbol{z}/R_c,\ t/t_c)\\&=\phi(|\nu|^{1/2}\boldsymbol{z},\ \nu^2 t)\,.\end{aligned} \tag{B·1}$$

Furthermore, it is generally expected that a characteristic amplitude scale of ϕ also appears near the instability point. Thus the expression (B·1) has to be generalized as

$$\phi = |\nu|^x \tilde{\phi}(|\nu|^{1/2} z, \nu^2 t), \tag{B·2}$$

where x is assumed to be some positive constant determined later. The expression (B·2) enables us to estimate the order of magnitude of various terms appearing on the right-hand side of Eq. (2·24). This immediately leads to the conclusion that the most dominant nonlinear term is $(\nabla\phi)^2$ which is of the order of $|\nu|^{1+2x}$, and that the most dominant linear terms are $\nu\nabla^2\phi$ and $\nabla^2\nabla^2\phi$ which are of the order of $|\nu|^{2+x}$. Taking only the above three terms into account, we obtain Eq. (2·26). Since the linear growth of the phase disturbance must be suppressed by the nonlinear effect, the corresponding balance condition implies

$$|\nu|^{1+2x} = |\nu|^{2+x}, \tag{B·3}$$

namely, $x=1$.

References

1) Y. Kuramoto and T. Yamada, Prog, Theor. Phys. **56** (1976), 679.
2) T. Yamada and Y. Kuramoto, Prog. Theor. Phys. **56** (1976), 681.
3) O. E. Rössler, Z. Naturforsch. **31a** (1976), 1168.
4) O. E. Rössler, *Synergetics,* ed. by H. Haken (Springer, Berlin, Heidelberg and New York, 1977).
5) H. Yamazaki, Y. Oono and K. Hirakawa, J. Phys. Soc. Japan **44** (1978), 335.
6) H. Yamazaki, Y. Oono and K. Hirakawa, to appear in J. Phys. Soc. Japan (1978).
7) L. F. Olsen and H. Degn, Nature **267** (1977), 177.
8) R. A. Schmitz, K. R. Graziani and J. L. Hudson, J. Chem. Phys. **67** (1977), 3040.
9) O. E. Rössler and K. Wegmann, Nature, **271** (1978), 89.
10) See for instance, P. Glansdorff and I. Prigogine, *Thermodynamic Theory of Structure, Stability and Fluctuations* (Interscience, New York, 1971).
11) P. Ortoleva and J. Ross, J. Chem. Phys. **58** (1973), 5673.
12) Y. Kuramoto, *Synergetics,* ed. by H. Haken (Springer, Brelin, Heidelberg and New York, 1977).
13) H. Haken, *Synergetics,* ed. by H. Haken (Springer, Berlin, Heidelberg and New York, 1977).
14) N. Kopell and L. Howard, Studies in Appl. Math. **52** (1973), 291.
15) H. L. Swinney, P. R. Fenstermacher and J. P. Gollub, *Synergetics,* ed. by H. Haken (Springer, Berlin, Heidelberg and New York, 1977).
16) P. R. Fenstermacher, H. L. Swinney, S. V. Benson and J. P. Gollub, *Bifurcation Theory and Applications in Scientific Disciplines,* ed. by O. Gurel and O. E. Rössler (New York Academy of Sciences, 1978).
17) A. C. Newell and J. A. Whitehead, J. Fluid. Mech. **38** (1969), 279.
18) Y. Kuramoto and T. Tsuzuki, Prog. Theor. Phys. **52** (1974), 1399.
19) Y. Kuramoto and T. Tsuzuki, Prog. Theor. Phys. **54** (1975), 687.
20) A. Wunderlin and H. Haken, Z. Phys. **B21** (1975), 393.
21) H. Haken, Z. Phys. **B20** (1975), 413.
22) H. Haken, Z. Phys. **B21** (1975), 105.
23) L. D. Landau and E. M. Lifshitz, *Fluid Mechanics* (Pergamon Press, Oxford, 1975).

24) D. D. Joseph, *Stability of Fluid Motions* (Springer, Berlin, and New York, 1976).
25) E. N. Lorenz, J. Atm. Sci. **20** (1963), 130.
26) I. Shimada and T. Nagashima, Prog. Theor. Phys. **59** (1978), 1033.
27) O. E. Rössler, *Bifurcation Theory and Applications in Scientific Disciplines,* ed. by O. Gurel and O. E. Rössler (New York Academy of Science, 1978).
28) T. Yamada and H. Fujisaka, Z. Phys. **B28** (1977), 239.

Discussion

G. Nicolis: In the case of phase turbulence, you mentioned an interesting dependence on the system sise. Presumably, what happens is that as L increases the number of linearly unstable modes gets large. We know, however, that all modes except that corresponding to the first bifurcation emerge as unstable solutions. Do you have evidence of secondary or higher bifurcations stabilizing these modes (and leading, presumably, to quasiperiodic solution) before the transition to chaos takes place?

Y. Kuramoto: My system shows successive bifurcations as the number of linearly unstable modes increases as I discussed in my talk. However, the point of higher bifurcation does not in general coincide with the point at which the number of linearly unstable modes is increased by one.

D. Broomhead: In your discussion of "phase chaos" you commented that you still did not understand its origin and yet your results apparently conform well with the currently held view on turbulence. Increasing the system size introduces first one, then two and three frequencies, each associated with an unstable mode. Concomitant with this the behavior changes from periodic to quasiperiodic, associated with a 2-torus, and finally with the possibility of a 3-torus it becomes chaotic. Could you please say what it is that doesn't convince you about this view?

Y. Kuramoto: Since my system has a translational symmetry the first unstable mode can completely be eliminated if we work with a suitable moving frame of reference, so that the first frequency ω_1 cannot be regarded as a nontrivial fundamental frequency. This is one of the reasons why I cannot find the connection of my phase turbulence with the prediction by Ruelle and Takens.

H. Haken: Since your system has finite length there is a discrete number of modes. How many modes did you take into account explicitly?

Y. Kuramoto: In my numerical calculation I have explicitly taken into account 15∼30 modes.

Y. Sawada: You have said, if I remember correctly, that when the concentration gradient is small you have phase turbulence and that when it is bigger you have amplitude turbulence. My limited experience tells me that we usually have pseudo wave in the former case and that we have trigger wave in the latter case. Could you tell me the condition for the occurence of your turbulence?

Y. Kuramoto: Phase turbulence is in general a turbulence with slowly varying concentration in space. In that case we have, in a way, chaotic phase waves. The condition for the appearence of phase turbulence is $\nu<0$. As ν decreases further, the amplitude variation becomes non-negligible, and the chaotic behavior then comes to have quite a new feature, namely, the feature of the amplitude turbulence. Whether or not the resulting chaotic waves may be called chaotic trigger waves or not depends on specific character of oscillation.